Theory of Ion Cyclotron Resonance Power Absorption for Nonreactive and Reactive Ions

Katsuyuki AOYAGI[1)]

Faculty of Engineering, Hokkaido University, Sapporo 060

(Received March 22, 1973)

An exact solution of the equation of motion and exact expressions of the ion current in ion cyclotron resonance power absorption were obtained. Instantaneous and total power absorptions together with power absorption line shapes were derived. Ion current expressions were also derived for both nonreactive and reactive ions over the whole range of pressure. The results agreed with those obtained previously for high and low pressures with appropriate approximation. The rate constants for the disappearance of primary ions and for the formation of nonreactive secondary ions were obtained from the ion cyclotron resonance experiments. The results showed good agreement with those obtained by other methods.

A charged particle moving in a strong uniform magnetic field describes a helical orbit which is a combination of a translation along a field line and a circular motion in a plane perpendicular to the direction of the magnetic field. The motion along the magnetic field is independent of the strength of the magnetic field. The circular motion in the plane is independent of the translational motion along the field lines. The angular frequency or cyclotron frequency ω of the circular motion is independent of the velocity of the ion and is given by

$$\omega = \frac{e\mathbf{H}}{mc}, \tag{1}$$

where e is the charge of the particle, $\mathbf{H}$ the magnetic field strength, m the particle mass, and c the velocity of light.[2)]

If a sinusoidal time-varying electric field $\mathbf{E}(t)$ with the frequency ω_1 is applied perpendicular to a static magnetic field $\mathbf{H}$, and the magnetic field is swept, the ion resonates at $\omega=\omega_1$ and absorbs energy from the sinusoidal time-varying electric field. The ion is accelerated and the radius of its orbit increases with time. An absorption of energy by the ions can be readily observed by a marginal oscillator detector[3,4)] or a bridge detector.[5,6)] With a fixed observing frequency, a spectrum obtained by sweeping the magnetic field is linear in the mass.

In the average chemically nonreactive ion undergoing ion cyclotron resonance, the phenomenological equation of motion for an ion is given by[5,9)]

$$\frac{d\mathbf{v}}{dt} = \frac{e}{m}\mathbf{E}(t) + \frac{e}{mc}\mathbf{v}\times\mathbf{H} - \xi\mathbf{v}, \tag{2}$$

where $\mathbf{v}$ is the nonrandom part of the average ion velocity, and ξ the reduced collision frequency that specifies the rate of momentum relaxation of the ion. If the ion undergoes only elastic collisions with the neutral species, the reduced collision frequency is given by[10)]

$$\xi = \frac{nm}{m+M}\langle v\sigma_d(v)\rangle, \tag{3}$$

where n and M are the number density and mass of the neutral species, respectively, and $\sigma_d(v)$ and v are the diffusion cross section and relative velocity of the ion to the neutral pair, respectively. The angle bracket indicates an average over the distribution of relative velocities.

Wobschall *et al.*[5)] and Beauchamp[9)] obtained a steady-state solution of Eq. (2) which leads to the Lorentzian line-shape expression for power absorption. The steady-state power absorption of an ion results in the broadening of ion cyclotron resonance (ICR) line shapes in the high-pressure limit where many collision occur during the ion transit time. The steady-state theory assumes equilibrium between power absorption and collision dissipation, ignoring the transient effect. However, it has been successfully applied to the determination of the collision frequency or the nonreactive cross section of ions from the line-shapes.[5,9)] Beauchamp[5)] and Buttrill[11)] obtained an approximated solution of Eq. (2) for the case $\xi=0$, which leads to an expression for low-pressure power absorption. Line-shapes calculated from the low-pressure theory show good agreement with experimental results at low pressure.[11)] In the presence of ion-molecule reactions, the theory has been extended successfully for determining of ion-molecule reaction rates using ICR signal intensity. The calculated rates show a substantial agreement with those measured by other techniques.[12)]

Recently, a more general solution for the phenomenological equation of motion of an ion in the ICR cell has been given by Comisarow[10)] and Dunbar[13)] which bridges the gap between the low- and high-pressure theories. This "total-pressure theory" has clarified the power absorption expressions for the chemically reactive ions.[10)] The theory has also been used for obtaining the collision relaxation rate and substantial probability for charge transfer by transient ICR experiment.[13)] However, in this theory, the ion current expression is not treated in detail.

In this paper, we propose exact expressions of ion current in the ICR cell, and an exact solution of the phenomenological equation of motion for the velocity of an ion used for deriving the power absorption of an ion and the ion kinetics. The ion-molecule reaction rate constants for the disappearance of primary ions and for the formation of nonreactive secondary ions are determined from ion cyclotron single resonance (ICSR) spectra. Rate constants are compared with values obtained by other methods. Close agreement between the present and previous values was obtained.

Theory

Ion Motion in the ICR Cell. The Cartesian coordinate system is chosen so that the static magnetic field is parallel to the z axis, the electrostatic drift field and the rf electric field are parallel to the x axis, and the ions drift to the y axis. Then ion motion in the x-y plane is independent of motion in the z direction.

The electrostatic trapping field is parallel to the z axis, as usually employed in the ICR cell.[3] The trapping field should not affect the power absorption of an ion.[3] The trapping voltage, however, shifts the ion cyclotron resonance frequency.[14,16] In the ICR cell, the electrostatic drift field only determines the residence time of the center of guide of the circular motion for an ion in the absence of collision.[3]

The actual motion of the ion in the analyzer region of the ICR cell consists of different types motion. A circular motion due to the Lorentz force in the x-y plane with increasing orbit radius with time, in which the ion absorbs energy from the applied rf electric field, and a motion of drift at constant velocity along the $-y$ axis lead to a trochoidal motion of increasing radius in the x-y plane. Furthermore, the ion describes an executed harmonic motion in a parabolic potential field in the x-z plane between the trapping electrodes. The exact solution of Eq. (2) leads to the above complicated motion of the ion in the analyzer region of the ICR cell.

Solution of Equation of Motion. In the absence of reactive collisions, the motion of an ion in the ICR cell can be described by Eq. (2). In the ICR cell, homogeneous electric and magnetic field distributions are assumed, the following electric and magnetic field configurations also being assumed:

$$\mathbf{H} = H_0\boldsymbol{k}, \tag{4}$$

$$\mathbf{E} = E_d\boldsymbol{i} + E_1 \sin(\omega_1 t+\phi_1)\boldsymbol{i} + E_t\boldsymbol{k}, \tag{5}$$

where H_0 is the static magnetic field strength, $\boldsymbol{i}$, $\boldsymbol{j}$, and $\boldsymbol{k}$ unit vectors of the coordinate system, E_d is the electrostatic drift field strength, E_t a function of z giving the electrostatic trapping field strength, and E_1 the observed rf electric field strength from the marginal oscillator or the oscillator for the bridge with frequency ω_1. The phase factor of ϕ_1 has been introduced because the rf phase at $t=0$ is not fixed.

Equation (2) is now separated into an equation of v_z only and two coupled equations of v_x and v_y. The relevant equations of motion are then;

$$\frac{dv_x}{dt} = \frac{e}{m}[E_d+E_1 \sin(\omega_1 t+\phi_1)] + \omega v_y - \xi v_x, \tag{6a}$$

$$\frac{dv_y}{dt} = -\omega v_x - \xi v_y. \tag{6b}$$

In the present investigation, the motion in the z direction does not affect the power absorption and will not be considered further.

An ion whose initial velosity v_0 is due to the thermal velocity leads to a circular motion with phase angle ϕ_0, $v_x(0)=-v_0\cos\phi_0$ and $v_y(0)=v_0\sin\phi_0$ at $t=0$. The exact solution of Eq. (6) is given by[7]

$$\begin{aligned} v_x = {} & v_0 \sin(\omega t-\phi_0)\exp(-\xi t) \\ & + \frac{eE_d}{m}\left[\frac{\xi-(\xi\cos\omega t-\omega\sin\omega t)\exp(-\xi t)}{\omega^2+\xi^2}\right] \\ & + \frac{eE_1}{m}\{A\sin(\omega_1 t+\phi_1)-B\cos(\omega_1 t+\phi_1) \\ & - [(C\cos\phi_1+D\sin\phi_1)\sin\omega t \\ & - (B\cos\phi_1-A\sin\phi_1)\cos\omega t]\exp(-\xi t)\}, \end{aligned} \tag{7a}$$

$$\begin{aligned} v_y = {} & v_0 \cos(\omega t-\phi_0)\exp(-\xi t) \\ & + \frac{eE_d}{m}\left[\frac{\omega-(\xi\sin\omega t+\omega\cos\omega t)\exp(-\xi t)}{\omega^2+\xi^2}\right] \\ & + \frac{eE_1}{m}\{D\sin(\omega_1 t+\phi_1)+C\cos(\omega_1 t+\phi_1) \\ & - [(B\cos\phi_1-A\sin\phi_1)\sin\omega t \\ & + (C\cos\phi_1+D\sin\phi_1)\cos\omega t]\exp(-\xi t)\}, \end{aligned} \tag{7b}$$

where

$$\begin{aligned} A &= [\xi(\xi^2+\omega_1^2-\omega^2)+2\xi\omega^2]/F, \\ B &= \omega_1(\xi^2+\omega_1^2-\omega^2)/F, \\ C &= 2\xi\omega\omega_1/F, \\ D &= [\omega(\xi^2+\omega_1^2-\omega^2)-2\xi^2\omega]/F, \\ F &= [(\omega_1-\omega)^2+\xi^2][(\omega_1+\omega)^2+\xi^2]. \end{aligned}$$

Line Shape Expression for Nonreactive Ion. a) Power Absorption of an Average Nonreactive Ion: Power absorption A of an ion from the rf electric field is given by

$$A = \langle e\mathbf{E}(t)\cdot\mathbf{v}(t)\rangle = eE_1 v_x \sin(\omega_1 t+\phi_1), \tag{8}$$

where v_x represents only the third term of Eq. (7a), because there is no observed effect of either the drift field or the initial velocity of an ion on the power absorption. The third term of Eq. (7b) has an effect on the power dispersion for an ion. The initial velocity of an ion with phase angle ϕ_0 will not contribute to the actual power absorption. Since an ensemble of ions enters the analyzer region in the ICR cell at time dt, the phase angles are expected to be distributed randomly so that the average over a period is 0.

Substituting the third term of Eq. (7a) into Eq. (8), the power absorption can be obtained by averaging over the phase angle ϕ_1 since all values of ϕ_1 are equally probable. With the approximation that

$$\omega_1 + \omega \approx 2\omega, \tag{9}$$

$$\xi \ll \omega_1, \tag{10}$$

the instantaneous power absorption by an ion is found to be

$$\begin{aligned} A(\omega_1=\omega) = {} & \frac{e^2E_1^2}{4m[(\omega_1-\omega)^2+\xi^2]}\{\xi+[(\omega_1-\omega)\sin(\omega_1-\omega)t \\ & -\xi\cos(\omega_1-\omega)t]\exp(-\xi t)\}, \end{aligned} \tag{11}$$

which is a function of t, ω, ω_1, and ξ. The first term is a steady-state power absorption observed under slow passage conditions. The second term is a transient term of a damped oscillation with frequency $|\omega_1-\omega|$, giving the ICR heterodyne spectrum.[13] The absorption giving by Eq. (11) agrees with that of Comisarow[10] and that of Dunber[13] who used slightly different methods.

At resonance $\omega_1=\omega$, the instantaneous power absorption is shown to be

$$A(\omega_1=\omega) = \frac{e^2E_1^2}{4m\xi}[1-\exp(-\xi t)]. \quad (12)$$

If the pressure is sufficiently high for each ion to suffer many nonreactive collisions, Eq. (11) is reduced to

$$A(\xi t \gg 1) = \frac{e^2E_1^2}{4m}\frac{\xi}{(\omega_1-\omega)^2+\xi^2} \quad (13)$$

by application of the approximation

$$\xi t \gg 1. \quad (14)$$

This high-pressure power absorption represents the Lorentzian line shape and agrees with the results of Beauchamp[9] and Comisarow.[10] In the collisionless limit $\xi \to 0$, Eq. (11) is reduced to

$$A(\xi \to 0) = \frac{e^2E_1^2}{4m(\omega_1-\omega)}\sin(\omega_1-\omega)t. \quad (15)$$

This low-pressure power absorption agrees with that of Beauchamp,[9] of Buttrill[11] and also of Comisarow.[10]

b) Total Power Absorption for Nonreactive Ion: Under idealized experimental ICR conditions, the homogeneous electric and magnetic field distributions are assumed in the ICR cell. Ions are produced in a source region with electron impact at a rate n_0 ions per second, and then drift through an anlyzer region at constant drift velocity. It has been assumed that the distribution of ions is uniform inside the ICR cell. There is a constant number $n_0\tau$ of ions in time τ for an ion drift through the analyzer, each absorbing energy at the rate given in Eq. (11). Thus the total power absorption $A(T)$ is obtained by averaging the integration from 0 to τ, the time required for the ions to absorb energy from the applied rf electric field. The averaged total power absorption is given by

$$A(T) = \frac{1}{\tau}\int_0^\tau n_0\tau A(\omega_1=\omega)\mathrm{d}t$$

$$= \frac{n_0e^2E_1^2}{4m[(\omega_1-\omega)^2+\xi^2]}\left\{\xi\tau+\frac{(\omega_1-\omega)^2-\xi^2}{(\omega_1-\omega)^2+\xi^2}\right.$$

$$+\left[\frac{\{\xi^2-(\omega_1-\omega)^2\}\cos(\omega_1-\omega)\tau-2\xi(\omega_1-\omega)\sin(\omega_1-\omega)\tau}{(\omega_1-\omega)^2+\xi^2}\right]$$

$$\left.\times\exp(-\xi\tau)\right\}, \quad \text{for } \omega_1=\omega, \quad (16a)$$

and

$$A(T) = \frac{n_0e^2E_1^2}{4m\xi}\left\{1-\frac{1}{\xi\tau}[1-\exp(-\xi\tau)]\right\} \quad \text{for } \omega=\omega_1. \quad (16b)$$

Application of (14) in Eq. (16a) gives

$$A(T, \text{High-pressure}) = \frac{n_0e^2E_1^2\tau}{4m}\frac{\xi}{(\omega_1-\omega)^2+\xi^2}. \quad (17)$$

This represents the average total high-pressure power absorption expression.

In the collisionless limit $\xi \to 0$, Eq. (16a) is reduced to

$$A(T, \xi \to 0) = \frac{n_0e^2E_1^2}{4m(\omega_1-\omega)^2}[1-\cos(\omega_1-\omega)]. \quad (18)$$

The line shapes of ICR total power absorption for an ensemble of ions are represented by Eqs. (16)—(18). The results agree with those of Comisarow.[10]

Line Shape Expression for Reactive Ion. a) Ion Current in the Analyzer Region: When the pressure in the ICR cell is so high that the reactive collision cannot be ignored, ion-molecule reactions occur. In special cases where all ion-molecule collisions are reactive, the calculation of power absorption is particularly simple, since the reactive collision removes the ion as a power-absorption entity. Here, only one species of neutral reactant molecule is present assuming that no two ions formed in different steps have the same mass.

The cross section of ion-molecule reaction is the function of ion velocity. The thermal reaction cross section σ_θ can be estimated from the corresponding rate constant, and is given by[17]

$$\sigma_\theta = \frac{k}{v_\theta}, \quad (19)$$

where v_θ is the average thermal velocity of the reactant ion. The reaction cross section of ion-molecule reaction is also given by[18]

$$\sigma = \frac{S}{P_0Ml}, \quad (20)$$

where P_0 is the rate of primary ion formation in the electron beam, S the total secondary ion current after the primary ion has traveled a distance l from the origin (the electron beam), and M the neutral reactant molecule. In the source region, the angular velocity of the ion is almost equal to its thermal velocity, but is not the same at resonance in the analyzer region. Similarly, the path lengths of the ions in the source and analyzer regions are not the same. Thus, the cross sections of ion-molecule reaction in the source and in the anlyzer regions are not the same, the rate constants in the source and anlyzer regions also being different.

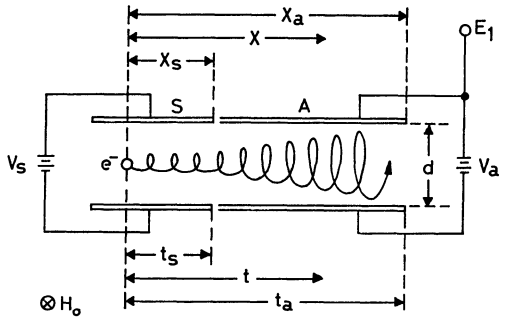

Fig. 1. Side view of the ICR cell showing parameters for kinetic analysis. e^- indicates the location of electron beam which forms the primary ions. The distances x_s, x and x_a are defined by the figure. t_s and t_a are the drift times through the source S and analyzer A regions, respectively.

Figure 1 shows a side cross-sectional view of the ICR cell required for kinetic analysis. Ions are produced in the source region by electron impact which are then made to drift through the analyzer region by the effect of the electrostatic drift field. Drift voltages are applied to the source and analyzer regions of the ICR cell separately. The time at each point x in the analyzer region, which is associated with the drift time t from the electron beam, is given by

$$t = \frac{x_s}{v_s} + \frac{x-x_s}{v_a}, \quad (21a)$$

where x_s and x are the distances indicated in Fig. 1, and v_s and v_a the drift velocities in the source and analyzer regions, respectively. The source exit time t_s and the analyzer exit time t_a for an ion are respectively given by

$$t_s = \frac{v_s}{v_{ds}} = \frac{x_s Hd}{cV_s} \tag{21b}$$

and

$$t_a = t_s + \frac{x_a - x_s}{v_{da}} = t_s + \frac{(x_a - x_s)Hd}{cV_a}, \tag{21c}$$

where V_s and V_a are the source drift and analyzer drift voltages, respectively. x_s, x_a, and d are the parameters defined in Fig. 1.

The equations for the change of ion current with time in the analyzer region are derived for the following primary, secondary, and tertiary chemical systems:[19,20]

Primary ion,

$$M + e^- \longrightarrow P^+, \tag{22}$$

Source-Formed Nonreactive Secondary (*SFNS*) ion,

$$P^+ + M \xrightarrow{k_{ps}} S_n^+ + N, \tag{23a}$$

Analyzer-Formed Nonreactive Secondary (*AFNS*) ion,

$$P^+ + M \xrightarrow{k_{pa}} S_n^+ + N, \tag{23b}$$

Source-Formed Reactive Secondary (*SFRS*) ion,

$$P^+ + M \xrightarrow{k_{ps},\, k_{ss}} S^+ + N, \tag{24a}$$

Analyzer-Formed Reactive Secondary (*AFRS*) ion,

$$P^+ + M \xrightarrow{k_{pa},\, k_{sa}} S^+ + N, \tag{24b}$$

Source-Formed Nonreactive Tertiary (*SFNT*) ion,

$$S^+ + M \xrightarrow{k_{ss}} T_n^+ + N, \tag{25a}$$

Analyzer-Formed Nonreactive Tertiary (*AFNT*) ion,

$$S^+ + M \xrightarrow{k_{sa}} T_n^+ + N. \tag{25b}$$

These obey the following equations in the analyzer region:

$$\frac{dP(t)_a}{d(t-t_{ps})} = -nk_{pa}P(t)_a, \tag{26}$$

$$\frac{dS(t)_{na}}{d(t-t_{ns})} = nk_{pa}P(t)_a, \tag{27}$$

$$\frac{dS(t)_a}{d(t-t_{ss})} = nk_{pa}P(t)_a - nk_{sa}S(t)_a, \tag{28}$$

$$\frac{dT(t)_a}{d(t-t_{ts})} = nk_{ss}S(t)_a. \tag{29}$$

The solutions are found to be

$$P(t)_a = P_0 \exp(-nk_{ps}t_{ps}) \exp[-nk_{pa}(t-t_{ps})], \tag{30}$$

$$S(SFNS, t)_a = P_0\{1 - \exp(-nk_{ps}t_{ns}) \times \exp[-nk_{pa}(t-t_{ns})]\}, \tag{31a}$$

$$S(AFNS, t)_a = P_0\{1 - \exp[-nk_{pa}(t-t_{ns})]\} \times \exp(-nk_{ps}t_{ns}), \tag{31b}$$

$$S(SFRS, t)_a = P_0\{(\alpha_s + \beta_s)\exp[-nk_{sa}(t-t_{ss})] - \alpha_s \exp[-nk_{pa}(t-t_{ss})]\}, \tag{32a}$$

$$S(AFRS, t)_a = P_0\alpha_s\{\exp[-nk_{sa}(t-t_{ss})] - \exp[-nk_{pa}(t-t_{ss})]\}, \tag{32b}$$

$$T(SFNT, t)_a = P_0\{1 - (\alpha_t + \beta_t)\exp[-nk_{sa}(t-t_{ts})] + \gamma_t \exp[-nk_{pa}(t-t_{ts})]\}, \tag{33a}$$

$$T(AFNT, t)_a = P_0\{\alpha_t + \beta_t + \gamma_t - (\alpha_t + \beta_t) \times \exp[-nk_{sa}(t-t_{ts})] + \gamma_t \exp[-nk_{pa}(t-t_{ts})]\}, \tag{33b}$$

where

$$\alpha_s = \frac{k_{pa}}{k_{pa} - k_{sa}} \exp(-nk_{ps}t_{ss}),$$

$$\beta_s = \frac{k_{ps}}{k_{ps} - k_{ss}}[\exp(-nk_{ss}t_{ss}) - \exp(-nk_{ps}t_{ss})],$$

$$\alpha_t = \frac{k_{pa}}{k_{pa} - k_{sa}} \exp(-nk_{ps}t_{ts}),$$

$$\beta_t = \frac{k_{ps}}{k_{ps} - k_{ss}}[\exp(-nk_{ss}t_{ts}) - \exp(-nk_{ps}t_{ts})],$$

$$\gamma_t = \frac{k_{sa}}{k_{pa} - k_{sa}} \exp(-nk_{ps}t_{ts}).$$

Here P_0 is the rate of primary ion formation in ions per second at the electron beam in the source region, n the number density of neutral reactant molecule, k_{ps} and k_{pa} are the ion-molecule reaction rates for the primary ion and k_{ss} and k_{sa} those for the secondary ion in the source and analyzer regions, respectively, and t_{ps}, t_{ns}, t_{ss}, and t_{ts} the source exit times of primary, nonreactive-secondary, reactive-secondary, and nonreactive-tertiary ions, respectively.

In the limits $k_{sa} \to 0$ and $k_{ss} \to 0$, Eq. (32a) is reduced to Eq. (31a). In the limit $k_{sa} \to 0$, Eq. (32b) is reduced to Eq. (31b).

Equations (30) and (31a) can be now rewritten in the following forms:

$$P(t)_{a1} = P_0 \exp[-nk_{pa}(t-t_{ps})] \quad \text{for } k_{pa} \gg k_{ps} \sim 0, \tag{34a}$$

$$P(t)_{a2} = \text{Eq. (30)} \quad \text{for } k_{pa} \neq k_{ps}, \tag{34b}$$

$$P(t)_{a3} = P_0 \exp(-nk_{pa}t_{ps}) \exp[-nk_{pa}(t-t_{ps})] \quad \text{for } k_{pa} \approx k_{ps}, \tag{34c}$$

$$S(SFNS, t)_{a1} = P_0 - P_0 \exp[-nk_{pa}(t-t_{ns})] \quad \text{for } k_{pa} \gg k_{ps} \sim 0, \tag{35a}$$

$$S(SFNS, t)_{a2} = \text{Eq. (31a)} \quad \text{for } k_{pa} \neq k_{ps}, \tag{35b}$$

$$S(SFNS, t)_{a3} = P_0 - P_0 \exp(-nk_{pa}t_{ns}) \times \exp[-nk_{pa}(t-t_{ns})] \quad \text{for } k_{pa} \approx k_{ps}. \tag{35c}$$

Eqs. (34a) and (35a), corresponding to the primary and nonreactive-secondary ion current expressions, have been reported in a slightly different form.[11,17]

b) Total Power Absorption for Primary Ions: Equation (11) can be rewritten in terms of t', the time an ion commences to absorb the power, and t'', the time an ion ceases to absorb the power in the analyzer region, as follows:

$$A(t''-t') = \frac{e^2E_1^2}{4m[(\omega_1-\omega)^2+\xi^2]} \times \{\xi + [(\omega_1-\omega)\sin(\omega_1-\omega)(t''-t') - \xi\cos(\omega_1-\omega)(t''-t')]\exp[-\xi(t''-t')]\}. \tag{36}$$

In the time $t-t_{ps}$ required for a primary ion to drift into the analyzer region, there are $P(t)_a\cdot(t-t_{ps})$ number of ions, each of which absorbs the energy at the rate given by Eq. (36). The total power absorption $A(T,P)$ is thus obtained by averaging the integration from t_{ps} to t_{pa}. The average total power absorption is given by

$$A(T,P)=\frac{1}{(t-t_{ps})}\int_{t_{ps}}^{t_{pa}}P(t)_a\cdot(t-t_{ps})\cdot A(t''-t')dt$$
$$=\frac{P_0e^2E_1^2\exp(-nk_{ps}t_{ps})}{4m_p[(\omega_1-\omega)^2+\xi_p^2]}F(p), \tag{37}$$

where

$$F(p)=\xi_pK_{1p}+K_{2p}-K_{3p}[K_{4p}\cos(\omega_1-\omega)(t_{pa}-t_{ps})$$
$$+K_{5p}\sin(\omega_1-\omega)(t_{pa}-t_{ps})],$$

m_p is the mass of the primary ion, t_{ps} and t_{pa} are the source exit and analyzer exit times, respectively, for the primary ion. $K_{1p}\sim K_{5p}$ are given in Appendix II. Equation (37) is the line shape expression of the total power absorption for the primary ions.

c) Total Power Absorption for Nonreactive Secondary Ions: In time $t-t_{ns}$ required for a nonreactive and stable secondary ion to drift into the analyzer region, there are $S(t)_{na}\cdot(t-t_{ns})$ number of ions, each of which absorbs energy at the rate given by Eq. (36). Thus the total power absorption $A(T,SFNS)$ due to source-formed nonreactive and stable secondary ions is given by averaging the integration from t_{ns} to t_{na}:

$$A(T,SFNS)=\frac{1}{(t-t_{ns})}\int_{t_{ns}}^{t_{na}}S(SFNS,t)_a\cdot(t-t_{ns})\cdot A(t''-t')dt$$
$$=\frac{P_0e^2E_1^2}{4m_n[(\omega_1-\omega)^2+\xi_n^2]}$$
$$\times\{f(NS)-F(NS)\exp(-nk_{ps}t_{ns})\}, \tag{38}$$

where

$$f(NS)=\xi_n(t_{na}-t_{ns})+N_{1n}$$
$$-N_{2n}[N_{3n}\cos(\omega_1-\omega)(t_{na}-t_{ns})$$
$$+N_{4n}\sin(\omega_1-\omega)(t_{na}-t_{ns})],$$
$$F(NS)=\xi_nK_{1n}+K_{2n}-K_{3n}[K_{4n}\cos(\omega_1-\omega)(t_{na}-t_{ns})$$
$$+K_{5n}\sin(\omega_1-\omega)(t_{na}-t_{ns})],$$

m_n is the mass of the nonreactive and stable secondary ion, t_{ns} and t_{na} are the source exit and analyzer exit times for the nonreactive and stable secondary ion, respectively. $N_{1n}\sim N_{4n}$ and $K_{1n}\sim K_{5n}$ are given in Appendix II.

Similarly, the total power absorption $A(T,AFNS)$ due to analyzer-formed nonreactive and stable secondary ions is given by averaging the integration from t_{ns} to t_{na}:

$$A(T,AFNS)=\frac{1}{(t-t_{ns})}\int_{t_{ns}}^{t_{na}}S(AFNS,t)_a\cdot(t-t_{ns})\cdot A(t''-t')dt$$
$$=\frac{P_0e^2E_1^2\exp(-nk_{ps}t_{ns})}{4m_n[(\omega_1-\omega)^2+\xi^2]}[f(NS)-F(NS)]. \tag{39}$$

Equations (38) and (39) are the line shape expressions of total power absorption for the source-formed and analyzer-formed nonreactive and stable secondary ions, respectively. The total power absorption due to nonreactive and stable secondary ions is given by the sum of Eqs. (38) and (39):

$$A(T,S_n)=A(T,SFNS)+A(T,AFNS)$$

d) Total Power Absorption for Reactive Secondary Ions: In time $t-t_{ns}$ required for a reactive secondary ion to drift into the analyzer region, there are $S(t)_a\cdot(t-t_{ns})$ number of ions, each of which absorbs energy at the rate given by Eq. (36). Thus the total power absorption $A(T,SFRS)$ due to source-formed reactive secondary ions is given by averaging the integration from t_{ss} to t_{sa}:

$$A(T,SFRS)=\frac{1}{(t-t_{ss})}\int_{t_{ss}}^{t_{sa}}S(SFRS,t)_a\cdot(t-t_{ss})\cdot A(t''-t')dt$$
$$=\frac{P_0e^2E_1^2}{4m_s[(\omega_1-\omega)^2+\xi_s^2]}[(\alpha_s+\beta_s)R(s)-\gamma_sF(s)], \tag{40}$$

where

$$R(s)=\xi_sR_{1s}+R_{2s}-R_{3s}[R_{4s}\cos(\omega_1-\omega)(t_{sa}-t_{ss})$$
$$+R_{5s}\sin(\omega_1-\omega)(t_{sa}-t_{ss})],$$
$$F(s)=\xi_sK_{1s}+K_{2s}-K_{3s}[K_{4s}\cos(\omega_1-\omega)(t_{sa}-t_{ss})$$
$$+K_{5s}\sin(\omega_1-\omega)(t_{sa}-t_{ss})],$$

m_s is the mass of the reactive secondary ion, t_{ss} and t_{sa} are the source exit and analyzer exit times of the reactive secondary ion, respectively. $R_{1s}\sim R_{5s}$ and $K_{1s}\sim K_{5s}$ are given in Appendix II.

Similarly, the total power absorption $A(T,AFRS)$ due to analyzer-formed reactive secondary ions is given by averaging the integration from t_{ss} to t_{sa}:

$$A(T,AFRS)=\frac{1}{(t-t_{ss})}\int_{t_{ss}}^{t_{sa}}S(AFRS,t)_a\cdot(t-t_{ss})\cdot A(t''-t')dt$$
$$=\frac{P_0e^2E_1^2\alpha_s}{4m_s[(\omega_1-\omega)^2+\xi_s^2]}[R(s)-F(s)]. \tag{41}$$

Equation (40) and (41) are the line shape expressions of total power absorption for the source-formed and analyzer-formed reactive secondary ions, respectively. The total power absorption due to reactive secondary ions is given by the sum of Eqs. (40) and (41):

$$A(T,S)=A(T,SFNS)+A(T,AFRS).$$

In the limits $k_{sa}\to 0$ and $k_{ss}\to 0$, Eq. (40) is reduced to Eq. (38). In the limit $k_{sa}\to 0$, Eq. (41) is reduced to Eq. (39).

e) Total Power Absorption for Nonreactive Tertiary Ions: In time $t-t_{ts}$ required for a nonreactive and stable tertiary ion to drift into the analyzer region, there are $T(t)_a\cdot(t-t_{ts})$ number of ions, each of which absorbs energy at the rate given by Eq. (36). Thus the total power absorption $A(T,SFNT)$ due to source-formed nonreactive and stable tertiary ions is obtained by averaging the integration from t_{ts} to t_{ta}:

$$A(T,SFNT)=\frac{1}{(t-t_{ts})}\int_{t_{ts}}^{t_{ta}}T(SFNT,t)_a\cdot(t-t_{ts})\cdot A(t''-t')dt$$
$$=\frac{P_0e^2E_1^2}{4m_t[(\omega_1-\omega)^2+\xi_t^2]}$$
$$\times\{f(T)-(\alpha_t+\beta_t)R(T)+\gamma_tF(T)\}, \tag{42}$$

where

$$f(T)=\xi_t(t_{ta}-t_{ts})+N_{1t}-N_{2t}[N_{3t}\cos(\omega_1-\omega)(t_{ta}-t_{ts})$$
$$+N_{4t}\sin(\omega_1-\omega)(t_{ta}-t_{ts})],$$

$$R(T) = \xi_t R_{1t} + R_{2t} - R_{3t}[R_{4t}\cos(\omega_1-\omega)(t_{ta}-t_{ts}) + R_{5t}\sin(\omega_1-\omega)(t_{ta}-t_{ts})],$$
$$F(T) = \xi_t K_{1t} + K_{2t} - K_{3t}[K_{4t}\cos(\omega_1-\omega)(t_{ta}-t_{ts}) + K_{5t}\sin(\omega_1-\omega)(t_{ta}-t_{ts})],$$

m_t is the mass of the nonreactive and stable tertiary ion, t_{ts} and t_{ta} are the source exit and analyzer exit times of the nonreactive and stable tertiary ion, respectively. $N_{1t}\sim N_{4t}$, $R_{1t}\sim R_{5t}$, and $K_{1t}\sim K_{5t}$ are given in Appendix II.

Similarly, the total power absorption $A(T,AFNT)$ due to analyzer-formed nonreactive and stable tertiary ions is given by averaging the integration from t_{ts} to t_{ta}:

$$A(T,AFNT) = \frac{1}{(t-t_{ts})}\int_{t_{ts}}^{t_{ta}} T(AFNT,t)_a\cdot(t-t_{ts})\cdot A(t''-t')dt$$
$$= \frac{P_0e^2E_1^2}{4m_t[(\omega_1-\omega)^2+\xi_t^2]}\{(\alpha_t+\beta_t+\gamma_t)f(T) - (\alpha_t+\beta_t)R(T)+\gamma_t F(T)\}. \quad (43)$$

Equations (42) and (43) are the line shape expressions of total power absorption for the source-formed and analyzer-formed nonreactive and stable tertiary ions, respectively. The total power absorption due to nonreactive and stable tertiary ions is given by the sum of Eqs. (42) and (43):

$$A(T,T) = A(T,SFNT) + A(T,AFNT).$$

Intensity Formula at Resonance. *a) Primary Ion*: In general, a full line shape expression is not required for the experimental determination of rate constant. The formula required for the ICSR signal intensity for an ion-molecule reaction described by Eqs. (22)—(25), is given as follows:

Applying the limit $\omega_1\to\omega$ to Eq. (37), we obtain the following intensity equation for primary ions;

$$I(P) = \frac{P_0e^2E_1^2\exp(-nk_{ps}t_{ps})}{4m_p\xi_p}\left\{\frac{1-\exp[-nk_{pa}(t_{pa}-t_{ps})]}{nk_{pa}} - \frac{1-\exp[-(nk_{pa}+\xi_p)(t_{pa}-t_{ps})]}{nk_{pa}+\xi_p}\right\}. \quad (44)$$

Under the approximation $k_{pa}\approx k_{ps}$, the first term of Eq. (44) corresponds to the intensity equation with the primary ion.[19] The second term points out the disadvantage of the old treatment, since k_{pa} should not be equal to k_{ps}. Under the collisionless limit $\xi\to 0$ and approximation $k_{pa}\approx k_{ps}$, Eq. (44) agrees with the intensity equation.[11] It is worthwhile noting that in our case the term of collision frequency ξ_p does not appear in the third order expansion of Eq. (44), and that no effect of collision frequency on signal intensity is considered.

b) Nonreactive Secondary Ion: The limit $\omega_1\to\omega$ in Eqs. (38) and (39) gives the following intensity equations for source-formed and analyzer-formed nonreactive and stable secondary ions, respectively;

$$I(SFNS) = \frac{P_0e^2E_1^2}{4m_n\xi_n}\Big\langle(t_{na}-t_{ns}) - \frac{1-\exp[-\xi_n(t_{na}-t_{ns})]}{\xi_n} - \left\{\frac{1-\exp[-nk_{pa}(t_{na}-t_{ns})]}{nk_{pa}} - \frac{1-\exp[-(nk_{pa}+\xi_n)(t_{na}-t_{ns})]}{nk_{pa}+\xi_n}\right\} \times\exp(-nk_{ps}t_{ns})\Big\rangle, \quad (45)$$

and

$$I(AFNS) = \frac{P_0e^2E_1^2\exp(-nk_{ps}t_{ns})}{4m_n\xi_n}\left\{(t_{na}-t_{ns}) - \frac{1-\exp[-\xi_n(t_{na}-t_{ns})]}{\xi_n} - \frac{1-\exp[-nk_{pa}(t_{na}-t_{ns})]}{nk_{pa}} + \frac{1-\exp[-(nk_{pa}+\xi_n)(t_{na}-t_{ns})]}{nk_{pa}+\xi_n}\right\}. \quad (46)$$

In the collisionless limit $\xi\to 0$, we can obtain the intensity equations of collisionless limiting case for source-formed and analyzer-formed nonreactive secondary ions. Under the approximation $k_{pa}\approx k_{ps}$, the intensity equation for source-formed nonreactive ion of collisionless limiting case corresponds to the secondary ion intensity expression.[11] The limit $k_{ps}\to 0$, applied to Eq. (46) and collisionless limiting case of Eq. (46), gives Eq. (45) and the collisionless limiting case of Eq. (45), respectively.

c) Reactive Secondary Ion: The intensity equations for the source-formed and analyzer-formed reactive secondary ions were similarly calculated:

$$I(SFRS) = \frac{P_0e^2E_1^2}{4m_s\xi_s}\Big\langle\frac{(\alpha_s+\beta_s)\{1-\exp[-nk_{sa}(t_{sa}-t_{ss})]\}}{nk_{sa}} - \frac{\alpha_s\{1-\exp[-nk_{pa}(t_{sa}-t_{ss})]\}}{nk_{pa}} - \frac{(\alpha_s+\beta_s)\{1-\exp[-(nk_{sa}+\xi_s)(t_{sa}-t_{ss})]\}}{nk_{sa}+\xi_s} - \frac{\alpha_s\{1-\exp[-(nk_{pa}+\xi_s)(t_{sa}-t_{ss})]\}}{nk_{pa}+\xi_s}\Big\rangle, \quad (47)$$

and

$$I(AFRS) = \frac{P_0e^2E_1^2\alpha_s}{4m_s\xi_s}\left\{\frac{1-\exp[-nk_{sa}(t_{sa}-t_{ss})]}{nk_{sa}} - \frac{1-\exp[-(nk_{sa}+\xi_s)(t_{sa}-t_{ss})]}{nk_{sa}+\xi_s} - \frac{1-\exp[-nk_{pa}(t_{sa}-t_{ss})]}{nk_{pa}} + \frac{1-\exp[-(nk_{pa}+\xi_s)(t_{sa}-t_{ss})]}{nk_{pa}+\xi_s}\right\}. \quad (48)$$

In the expansion of Eqs. (47) and (48) with respect to ξ, we obtain intensity equations of collisionless limiting case for the source-formed and analyzer-formed reactive secondary ions, respectively.

d) Nonreactive Tertiary Ion: By a similar calculation the following intensity equations for source-formed and analyzer-formed nonreactive and stable tertiary ions are obtained.

$$I(SFNT) = \frac{P_0e^2E_1^2}{4m_t\xi_t}\Big\langle(t_{ta}-t_{ts}) - \frac{1-\exp[-\xi_t(t_{ta}-t_{ts})]}{\xi_t} - \frac{(\alpha_t+\beta_t)}{nk_{sa}}\{1-\exp[-nk_{sa}(t_{ta}-t_{ts})]\} + \frac{\gamma_t}{nk_{pa}}\{1-\exp[-nk_{pa}(t_{ta}-t_{ts})]\} + \frac{(\alpha_t+\beta_t)}{nk_{sa}+\xi_t}\{1-\exp[-(nk_{sa}+\xi_t)(t_{ta}-t_{ts})]\} - \frac{\gamma_t}{nk_{pa}+\xi_t}\{1-\exp[-(nk_{pa}+\xi_t)(t_{ta}+t_{ts})]\}\Big\rangle, \quad (49)$$

and

$$I(AFNT) = \frac{P_0e^2E_1^2}{4m_t\xi_t}\Big\langle(\alpha_t+\beta_t+\gamma_t)\Big\{(t_{ta}-t_{ts}) - \frac{1-\exp[-\xi_t(t_{ta}-t_{ts})]}{\xi_t}\Big\} - \frac{(\alpha_t-\beta_t)}{nk_{sa}}\{1-\exp[-nk_{sa}(t_{ta}-t_{ts})]\} + \frac{\gamma_t}{nk_{pa}}\{1-\exp[-nk_{pa}(t_{ta}-t_{ts})]\} + \frac{(\alpha_t+\beta_t)}{nk_{sa}+\xi_t}\{1-\exp[-(nk_{sa}+\xi_t)(t_{ta}-t_{ts})]\} - \frac{\gamma_t}{nk_{pa}+\xi_t}\{1-\exp[-(nk_{pa}+\xi_t)(t_{ta}-t_{ts})]\}\Big\rangle. \quad (50)$$

In the collisionless limit $\xi\to 0$ of Eqs. (49) and (50) which are expanded to third order with respect to ξ, we obtain the intensity equations of collisionless limiting case for the source-formed and analyzer-formed nonreactive tertiary ions.

Calculation of Rate Constant for the Disappearance of Primary Ions. In ion-molecule reactions, the power absorption due to the primary ion is decreased by the reactive collisions with neutral reactant molecules. The ion-molecule collision rate or reaction rate constant for disappearance of the primary ion can be obtained from Eq. (44). However, there is no effect of collision frequency on ICSR signal intensity. Thus, the collisionless limit $\xi\to 0$ is a fairly good approximation except at the high pressure where the collision broadening occurs.

Equation (44) can be now expanded to give

$$I(P_1, \xi\to 0) = \frac{P_0e^2E_1^2(t_{pa}-t_{ps})^2}{8m_p^2}[1-nk_{pa}(t_{pa}-t_{ps})] \quad \text{for } k_{pa}\gg k_{ps}\sim 0, \quad (51a)$$

$$I(P_2, \xi\to 0) = \frac{P_0e^2E_1^2}{8m_p^2}(t_{pa}-t_{ps})\Big\{(t_{pa}-t_{ps}) - \frac{n}{k_{pa}}[k_{pa}t_p-(k_{pa}-k_{ps})t_{ps}]^2\Big\} \quad \text{for } k_{pa}\neq k_{ps}, \quad (51b)$$

$$I(P_3, \xi\to 0) = \frac{P_0e^2E_1^2}{8m_p^2}(t_{pa}-t_{ps})[(t_{pa}-t_{ps})-nk_{pa}t_{pa}^2] \quad \text{for } k_{pa}\approx k_{ps}. \quad (51c)$$

Solving Eqs. (51a), (51b), and (51c) for k_{pa}, we have

$$k_{pa} = \frac{1}{n(t_{pa}-t_{ps})}\left[1-\frac{I(P_1, \xi\to 0)}{\alpha}\right] \quad \text{for } k_{pa}\gg k_{ps}\sim 0, \quad (52a)$$

$$k_{pa} = \frac{1}{n(t_{pa}-t_{ps})}\left[1-2nk_{ps}t_{ps}-\frac{I(P_2, \xi\to 0)}{\alpha}\right] \quad \text{for } k_{pa}\neq k_{ps}, \quad (52b)$$

and

$$k_{pa} = \frac{(t_{pa}-t_{ps})}{nt_{pa}^2}\left[1-\frac{I(P_3, \xi\to 0)}{\alpha}\right] \quad \text{for } k_{pa}\approx k_{ps}, \quad (52c)$$

where k_{pa} is the collision rate or the rate constant for the disappearance of the primary ions, and

$$\alpha = \frac{P_0e^2E_1^2}{8m_p^2}(t_{pa}-t_{ps})^2.$$

Calculation of Rate Constant for the Formation of Nonreactive Secondary Ions. Single-resonance spectra are usually obtained at constant rf frequency ω_1 by sweeping the magnetic field. The magnetic field at which an ion is in resonance is proportional to m/e as indicated by Eq. (1).

The source exit and analyzer exit times for the primary ion are given by Eqs. (21b) and (21c), respectively. The values of t_{ps} and t_{pa} are related by

$$t_{ns} = (m_n/m_p)t_{ps}, \quad (53a)$$

$$t_{ss} = (m_s/m_p)t_{ps}, \quad (53b)$$

$$t_{ts} = (m_t/m_p)t_{ps}, \quad (53c)$$

$$t_{na} = (m_n/m_p)t_{pa}, \quad (54a)$$

$$t_{sa} = (m_s/m_p)t_{pa}, \quad (54b)$$

and

$$t_{ta} = (m_t/m_p)t_{pa}. \quad (54c)$$

If $nk_it_j<1$, $(i, j=ps, pa, ns, na)$, then the exponentials in the collisionless limit of Eq. (44) can be expanded to the third order. Using Eqs. (53a) and (54a), they can be solved for k_{pa} giving the approximations:

$$k_{pa} = \frac{m_p^2I(NS, \xi\to 0)\cdot(t_{pa}-t_{ps})}{n[m_n^2I(P, \xi\to 0)\cdot\alpha_k+m_p^2I(NS, \xi\to 0)\cdot\beta_k]} \quad \text{for } k_{ps}\neq k_{pa}, \quad (55a)$$

$$k_{pa} = \frac{m_p^2I(NS, \xi\to 0)}{n[2m_n^2I(P, \xi\to 0)+m_p^2I(NS, \xi\to 0)](t_{pa}-t_{ps})} \quad \text{for } k_{pa}\gg k_{ps}\sim 0, \quad (55b)$$

and

$$k_{pa} = \frac{m_p^2I(NS, \xi\to 0)\cdot(t_{pa}-t_{ps})}{n\{m_n^2I(P, \xi\to 0)[2t_{pa}^2-(t_{pa}-t_{ps})t_{ps}]+m_p^2I(NS, \xi\to 0)t_{pa}^2\}} \quad \text{for } k_{pa}\approx k_{ps}, \quad (55c)$$

where

$$\alpha_k = 2(t_{pa}-t_{ps})^2 + \frac{3k_{ps}}{k_{pa}}(t_{pa}-t_{ps})t_{ps} + \frac{2k_{ps}^2}{k_{pa}^2}t_{ps}^2$$

and

$$\beta_k = (t_{pa}-t_{ps})^2 + \frac{2k_{ps}}{k_{pa}}(t_{pa}-t_{ps})t_{ps} + \frac{2k_{ps}^2}{k_{pa}^2}t_{ps}^2.$$

Under high pressure, if $nk_it_j<1$, $(i,j=pa, ps, na, ns)$, then exponentials in Eqs. (44), (45), and (46) can be expanded to fourth order. Using Eqs. (53a) and (54a), they can be solved for k_{pa} giving the approximations:

$$k_{pa} = \frac{m_p^2I(NS)[3-3nk_{ps}t_{ps}-\xi_p(t_{pa}-t_{ps})]-3m_n^2I(P)nk_{ps}t_{ps}}{2n[2m_n^2I(P)+m_p^2I(NS)](t_{pa}-t_{ps})} \quad \text{for } k_{ps}\neq k_{pa}, \quad (56a)$$

$$k_{pa} = \frac{m_p^2I(NS)[3-\xi_p(t_{pa}-t_{ps})]}{2n[2m_n^2I(P)+m_p^2I(NS)](t_{pa}-t_{ps})} \quad \text{for } k_{pa}\gg k_{ps}\sim 0, \quad (56b)$$

and

$$k_{pa} = \frac{m_p^2I(NS)[3-\xi_p(t_{pa}-t_{ps})]}{n[m_n^2I(P)\cdot(4t_{pa}-t_{ps})+m_p^2I(NS)\cdot(2t_{pa}+t_{ps})]} \quad \text{for } k_{ps}\approx k_{pa}. \quad (56c)$$

Equations (55a)—(56c) were derived on the assumption that a secondary ion does not suffer any reactive collisions in the resonance region of the ICR cell. If

a large fraction of secondary ions react with neutrals in the analyzer region, Eqs. (55a)—(56c) could not be applied. In this case, the rate constant for the formation of reactive secondary ion can be derived from Eqs. (44), (47), and (48).

Results and Discussion

Single- and Double-resonance Spectra. The ion-molecule reactions of acetonitrile have been studied by high-pressure mass spectrometry[21] and ICR spectroscopy.[22] Twenty-three ion-molecule reactions have been observed in acetonitrile by ICDR technique,[22] and the rate constants for the disappearance of ion-molecule reactions in acetonitrile has been measured with a time-of-flight mass spectrometer.[21]

Fig. 2. Single-resonance spectrum of acetonitrile at 60 eV electron energy and 1.1×10^{-5} Torr.

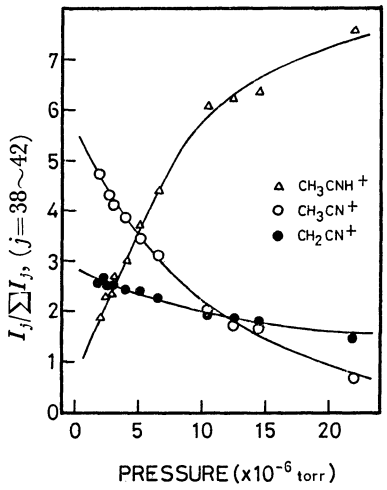

Fig. 3. Variation of single-resonance intensities of the various observed with pressure, at 60 eV electron energy.

However, the rate constant for the disappearance has not been reported by ICR spectroscopy. Equation (52) is applied to determine the rate constant for the disappearace of ions in acetonitrile.

Figure 2 shows a single-resonance spectrum of acetonitrile obtained at 1.1×10^{-5} Torr and electron energy of 60 eV. The spectrum is essentially the same as that reported.[22] The variations of single-resonance intensities with pressure are given in Fig. 3. The primary ion CH_2CN^+ and CH_3CN^+ decrease with increasing pressure. The secondary product CH_3CNH^+ increases with increasing pressure. The weak signal of $CHCN^+$ reaches a maximum, at around 6×10^{-6} Torr, and then decreases with increasing pressure. At a high electron energy, the sequence of reactions becomes complicated, probably because of possible generation of several reactant ions. By ICDR technique, however, one can readily identify the processes that produce each product ion. The ion-molecule reactions, identified by ICDR technique, are listed in Table 1. The results of ICDR experiments are in good agreement with those reported.[22]

Table 1. Ion-molecule reaction in acetonitrile

R1.	$C_2H_2^+$	+ CH_3CN	⟶	CH_3CNH^+	+ C_2H
R2.	HCN^+	+ CH_3CN	⟶	CH_3CNH^+	+ CN
R3.	H_2CN^+	+ CH_3CN	⟶	CH_3CNH^+	+ HCN
R4.	N_2H^+	+ CH_3CN	⟶	CH_3CNH^+	+ N_2
R5.	CH_2CN^+	+ CH_3CN	⟶	CH_3CNH^+	+ CHCN
R6.	CH_3CN^+	+ CH_3CN	⟶	CH_3CNH^+	+ CH_2CN
R7.	CH_2CN^+	+ CH_3CN	⟶	$C_3H_4CN^+$	+ HCN

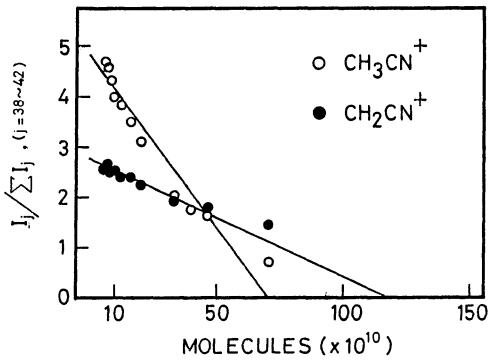

Fig. 4. $I_j/\sum I_j$, $(j=38—42)$, *vs.* number density of neutral reactant molecules for the reaction disappearing CH_3CN^+ with CH_3CN and for the reaction disappearing CH_2CN^+ with CH_3CN.

Determination of Rate Constant for the Disappearance of Primary Ion. From Eqs. (52a, b, c), it is evident that a plot of I *versus* n should give a straight line passing through a point (0, n) with a slope proportional to $1/k_{pa}$. The factor α is generally very small, and has been omitted in plotting Fig. 4. On the assumption that $k_{ps}\ll k_{pa}$, k_{ps} has been ignored in the calculation. Therefore, when $I=0$, Eq. (52a) is reduced to

$$k_{pa}(t_{pa}-t_{ps}) = 1/n,$$

where the source exit time t_{ps} and the analyzer exit time t_{pa} are given by Eqs. (21b) and (21c), respectively. The behavior of single-resonance signal intensities of primary ions CH_2CN^+ and CH_3CN^+ are interpreted by means of Eq. (52a).

The values of $k_{pa}(R5)=1.34\times10^{-9}$ and $k_{pa}(R6)=1.99\times10^{-9}$ cc mol^{-1} s^{-1} for the reactions (R5) and

(R6) obtained from Fig. 4 are in excellent agreement with previous values of $k(\mathrm{R5})=1.78\times10^{-9}$ and $k(\mathrm{R6})=2.01\times10^{-9}$ ml mol^{-1} s^{-1} determined by the conventional technique.[21]

Determination of Rate Constant for the Formation of Nonreactive Secondary Ion. In ion-molecule reactions of acetonitrile, CH_3CNH^+ is not essentially a nonreactive secondary ion. But tertiary ions formed from CH_3CNH^+ are so few that CH_3CNH^+ can be considered to be the nonreactive secondary ion.

In the limits $\xi\to0$ and $k_{ps}\to0$, it is evident that a plot of n *versus* $m_p{}^2I(NS,\ \xi\to0)/[2m_n{}^2I(P,\ \xi\to0)+m_p{}^2I(NS,\ \xi\to0)](t_{pa}-t_{ps})$ of Eq. (55) should give a straight line with a slope proportional to k_{pa} as shown in Fig. 5. The analysis supports the above results for reactions (R5) and (R6).

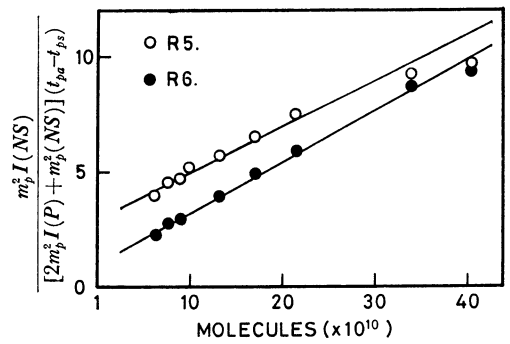

Fig. 5. $m^2{}_pI(NS)/[2m^2{}_nI(P)+m^2{}_pI(NS)](t_{pa}-t_{ps})$ *vs.* number density of neutral reactant molecules for the reaction of R(5) and for the reaction of R(6) listed in Table 1, respectively.

The values $k_{pa}(\mathrm{R5})=2.1\times10^{-9}$ and $k_{pa}(\mathrm{R6})=2.3\times10^{-9}$ cc mol^{-1} s^{-1} for reactions (R5) and (R6) are in very good agreement with previous results. Gupta *et al.*[23] reported $k(\mathrm{R6})=2.15\times10^{-9}$ cc mol^{-1} s^{-1} at 3.7 eV exit ion energy. Martin and Melton[24] reported $k(\mathrm{R6})=3.5\times10^{-9}$ cc mol^{-1} s^{-1} determined by conventional techniques. However, no value of k(R5) has been reported.

Experimental

The ICR spectra recorded with a JEOL JIC-3B spectrometer have been described in detail.[15] The ICR cell was of a three-section square type similar to the conventional one,[3] the grid electrode being added to improve the distribution of the electric field. Ions were produced in the source region by the electron impact and then forced to drift into the analyzer region where they were observed by a Twin-T bridge detector.[6] Single-resonance spectra were obtained in the field modulation mode, and double-resonance experiments were performed in the pulsed modulation mode.[8]

The experimental conditions were as follows: Energy of ionizing electrons=60 eV, source and analyzer drift field strengths=0.2 V/cm, trapping voltage=0.26 V, the observed rf electric field strength and frequency=0.02 V/cm and 100 kHz. Acetonitrile of reagent grade (Wako Pure Chem. Ind., Ltd.) was purified by trap-to-trap distillation before use. The sample was degassed under vacuum utilizing freeze-pump-thaw cycles.

The author would like to thank Professor Koichiro Hayashi for his encouragement, and Professor Junkichi Sohma for advice and discussions. The author is also indebted to Dr. Tetsuo Maruyama of JEOL (U.S.A.), INC. for his support, helpful suggestions and encouragement. The support of JEOL Co., Ltd. is gratefully acknowledged.

Appendix

I) Ion Kinetic Energy in the Absence of Collisions. Kinetic energy of an ion is also derived from Eq. (7) as follows.

$$W(\omega_1=\omega)=\frac{mv_0{}^2}{2}+\frac{v_0eE_1}{2}\left[t\cos(\phi_0+\phi_1)-\frac{1}{\omega}\sin\omega t\cos(\omega t-\phi_0+\phi_1)\right]+\frac{e^2E_1{}^2}{8m}\left[t^2+\frac{\sin^2\omega t}{\omega^2}-\frac{2t\sin\omega t\cos(\omega t+2\phi_1)}{\omega}\right]\quad\text{for }\omega_1=\omega.$$

If $\phi_0=0$ and $\phi_1=0$, the equation from which the oscillating terms are ignored agrees with that reported previously.[11]

II) List of Notations Used in the Text.

$K_{1p}=\{1-\exp[-nk_{pa}(t_{pa}-t_{ps})]\}/nk_{pa}$,
$K_{2p}=[(\omega_1-\omega)^2-\xi_p(nk_{pa}-\xi_p)]/[(nk_{pa}+\xi_p)^2+(\omega_1+\omega)^2]$,
$K_{3p}=\exp[-(nk_{pa}+\xi_p)(t_{pa}-t_{ps})]/[(nk_{pa}+\xi_p)^2+(\omega_1-\omega)^2]$,
$K_{4p}=(\omega_1-\omega)^2-\xi_p(nk_{pa}+\xi_p)$,
$K_{5p}=(\omega_1-\omega)(nk_{pa}+2\xi_p)$,
$N_{1n}=[(\omega_1-\omega)^2-\xi_n{}^2]/[(\omega_1-\omega)^2+\xi_n{}^2]$,
$N_{2n}=\exp[-\xi_n(t_{na}-t_{ns})]/[(\omega_1-\omega)^2+\xi_n{}^2]$,
$N_{3n}=(\omega_1-\omega)^2-\xi_n{}^2$,
$N_{4n}=2\xi_n(\omega_1-\omega)$,
$K_{1n}=\{1-\exp[-nk_{pa}(t_{na}-t_{ns})]\}/nk_{pa}$,
$K_{2n}=[(\omega_1-\omega)^2-\xi_n(nk_{pa}-\xi_n)]/[(nk_{pa}+\xi_n)^2+(\omega_1-\omega)^2]$,
$K_{3n}=\exp[-(nk_{pa}+\xi_n)(t_{na}-t_{ns})]/[(nk_{pa}+\xi_n]^2+(\omega_1-\omega)^2]$,
$K_{4n}=(\omega_1-\omega)^2-\xi_n(nk_{pa}+\xi_n)$,
$K_{5n}=(\omega_1-\omega)(nk_{pa}+2\xi_n)$,
$R_{1s}=\{1-\exp[-nk_{sa}(t_{sa}-t_{ss})]\}/nk_{sa}$,
$R_{2s}=[(\omega_1-\omega)^2-\xi_s(nk_{sa}+\xi_s)]/[(nk_{sa}+\xi_s)^2+(\omega_1-\omega)^2]$,
$R_{3s}=\exp[-(nk_{sa}+\xi_s)(t_{sa}-t_{ss})]/[(nk_{sa}+\xi_s)^2+(\omega_1-\omega)^2]$,
$R_{4s}=(\omega_1-\omega)^2-\xi_s(nk_{sa}+\xi_s)$,
$R_{5s}=(\omega_1-\omega)(nk_{sa}+2\xi_s)$,
$K_{1s}=\{1-\exp[-nk_{pa}(t_{sa}-t_{ss})]\}/nk_{pa}$,
$K_{2s}=[(\omega_1-\omega)^2-\xi_s(nk_{pa}+\xi_s)]/[(nk_{pa}+\xi_s)^2+(\omega_1-\omega)^2]$,
$K_{3s}=\exp[-(nk_{pa}+\xi_s)(t_{sa}-t_{ss})]/[(nk_{pa}+\xi_s)^2+(\omega_1-\omega)^2]$,
$K_{4s}=(\omega_1-\omega)^2-\xi_s(nk_{pa}+\xi_s)$,
$K_{5s}=(\omega_1-\omega)(nk_{pa}+2\xi_s)$,
$N_{1t}=[(\omega_1-\omega)^2-\xi_t{}^2]/[(\omega_1-\omega)^2+\xi_t{}^2]$,
$N_{2t}=\exp[-\xi_t(t_{ta}-t_{ts})]/[(\omega_1-\omega)^2+\xi_t{}^2]$,
$N_{3t}=(\omega_1-\omega)^2-\xi_t{}^2$,
$N_{4t}=2\xi_t(\omega_1-\omega)$,
$R_{1t}=\{1-\exp[-nk_{sa}(t_{ta}-t_{ts})]\}/nk_{sa}$,
$R_{2t}=[(\omega_1-\omega)^2-\xi_t(nk_{sa}+\xi_t)]/[(nk_{sa}+\xi_t)^2+(\omega_1-\omega)^2]$,

$$R_{3t} = \exp[-(nk_{sa}+\xi_t)(t_{ta}-t_{ts})]/[(nk_{sa}+\xi_t)^2+(\omega_1-\omega)^2],$$
$$R_{4t} = (\omega_1-\omega)^2 - \xi_t(nk_{sa}+\xi_t),$$
$$R_{5t} = (\omega_1-\omega)(nk_{sa}+2\xi_t),$$
$$K_{1t} = \{1-\exp[-nk_{pa}(t_{ta}-t_{ts})]\}/nk_{pa},$$
$$K_{2t} = [(\omega_1-\omega)^2-\xi_t(nk_{pa}+\xi_t)]/[(nk_{pa}+\xi_t)^2+(\omega_1-\omega)^2],$$
$$K_{3t} = \exp[-(nk_{pa}+\xi_t)(t_{ta}-t_{ts})]/[(nk_{pa}+\xi_t)^2+(\omega_1-\omega)^2],$$
$$K_{4t} = (\omega_1-\omega)^2 - \xi_t(nk_{pa}+\xi_t),$$
$$K_{5t} = (\omega_1-\omega)(nk_{pa}+2\xi_t).$$

References

1) JEOL Fellow, 1970–1972. On leave of absence from Division of Industrial Physical Chemistry, Faculty of Engineering, Hokkaido University, Sapporo 060. Present address: JEOL Co., Ltd. 1418 Nakagami, Akishima-shi, Tokyo 196

2) Gaussian CGS units are employed unless otherwise stated.

3) J. L. Beauchamp, L. R. Anders, and J. D. Baldeschwieler, *J. Amer. Chem. Soc.*, **89**, 4569 (1967).

4) K. Aoyagi, (a) *Bunseki-kiki.*, **10**, 703 (1972). (b) Unpublished data.

5) D. Wobschall, J. R. Graham, and D. P. Malone, *Phys. Rev.*, **131**, 1565 (1963).

6) K. Aoyagi, T. Miyamae, M. Irie, K. Hayashi, and J. Sohma, 5th Annual Conference on Applied Spectrometry., Tokyo (1969).

7) See, for example, K. Yoshida and T. Kato, "Ohyo-sugaku-1", Syokabo. Tokyo (1967).

8) K. Aoyagi, T. Miyamae, T. Seki, and S. Fujiwara, 4th Annual Conference on Applied Spectrometry., Tokyo (1968).

9) J. L. Beauchamp, *J. Chem. Phys.*, **46**, 1231 (1967).

10) M. B. Comisarow, *ibid.*, **55**, 205 (1971).

11) S. E. Buttrill, *ibid.*, **50**, 4125 (1969).

12) References 10, 11, 13, 17 and 19.

13) R. C. Dunbar, *J. Chem. Phys.*, **54**, 711 (1971).

14) S. Fujiwara, K. Aoyagi, and T. Miyamae, This Bulletin **43**, 561 (1970)

15) K. Aoyagi, K. Hayashi, and J. Sohma, *Bull. Fac. Eng. Hokkaido Univ.*, No. **62**, 65 (1971).

16) J. L. Beauchamp and J. T. Armstrong, *Rev. Sci. Instr.*, **40**, 123 (1969).

17) M. T. Bowers, D. D. Elleman, and J. King, *J. Chem. Phys.*, **50**, 4787 (1969).

18) J. M. S. Henis, *ibid.*, **52**, 282 (1970).

19) M. T. Bowers, D. D. Elleman, and J. L. Beauchamp, *J. Phys. Chem.*, **72**, 3599 (1968).

20) W. J. Moore, "Physical Chemistry," 3rd Ed, Maruzen Asian Edition, Maruzen Co., Ltd. (1962), p. 226.

21) J. L. Franklin, Y. Wada, P. Natalis, and P. M. Hierl, *J. Phys. Chem.*, **70**, 2353 (1966).

22) G. A. Gray, *J. Amer. Chem. Soc.*, **90**, 2177 (1968); *ibid.*, **90**, 6002 (1968).

23) S. K. Gupta, E. G. Jones, A. G. Harrison, and J. J. Myher, *Can. J. Chem.*, **45**, 3107 (1967).

24) T. W. Martin and C. E. Melton, *J. Chem. Phys.*, **32**, 700 (1960).